Efficient non-resonant absorption of electromagnetic radiation in thin cylindrical targets: experimental evidence

A. Akhmeteli[a], N.G. Kokodiy[b], B.V. Safronov[b], V.P. Balkashin[b], I.A. Priz[b] and A. Tarasevitch[c]

[a]LTASolid Inc., 10616 Meadowglen Ln 2708, Houston, TX 77042, USA;
[b]Kharkov National University, Ukraine, Kharkov, Svobody sq., 4;
[c]University of Duisburg-Essen, Institute of Experimental Physics, Lotharstr. 1, 47048 Duisburg, Germany

ABSTRACT

A theoretical possibility of non-resonant, fast, and efficient (up to 40 percent) heating of very thin conducting cylindrical targets by broad electromagnetic beams was predicted in [Akhmeteli, arXiv:physics/0405091 and 0611169] based on rigorous solution of the diffraction problem. The diameter of the cylinder can be orders of magnitude smaller than the wavelength (for the transverse geometry) or the beam waist (for the longitudinal geometry) of the electromagnetic radiation. Experimental confirmation of the above results is presented [Akhmeteli, Kokodiy, Safronov, Balkashin, Priz, Tarasevitch, arXiv:1109.1626 and 1208.0066].

Keywords: electromagnetic beams, efficient absorption, thin cylinder, diffraction

1. INTRODUCTION

In this experimental work, we show significant (up to 36%) absorption of broad electromagnetic beams in thin cylindrical targets (the diameter is two to three orders of magnitude less than the characteristic transverse dimension of the beam). This new physical effect can be used in numerous applications, including pumping of active media of short-wavelength lasers. For example, an exciting possibility of efficient heating of nanotubes by femtosecond laser pulses is discussed in Ref.[1] A theoretical possibility of non-resonant, fast, and efficient heating of extremely thin conducting cylindrical targets by broad electromagnetic beams was described in Ref.[2] (see also Refs.[1,3] and references there). In earlier work, either the conditions of efficient absorption in thin targets were resonant and thus difficult to use for practical plasma heating (Ref.[4]), or it was not noted that the power absorbed in a thin target can be comparable to the power in the incident wave (Refs.[5,6,7,8]).

The effect has the following physical mechanism: the absorption in the cylindrical target causes a deep fall in the field distribution, and this fall causes diffractive diffusion of the field towards the axis from a relatively large volume of the beam.

We consider two different geometries of target irradiation: the transverse geometry (Fig. 1) and the longitudinal geometry (Fig. 2).

2. TRANSVERSE GEOMETRY

Efficient heating takes place for converging axisymmetric cylindrical waves (under some limitations on the real part of the complex permittivity of the cylinder) if the diameter of the cylinder and the skin-depth are of the same order of magnitude and the electric field in the wave is directed along the common axis of the cylinder and the wave (see the exact conditions in Refs.[1,3] , where these conditions are derived based on a rigorous solution of the problem of diffraction of an electromagnetic beam on a cylinder). Similar conditions were derived earlier in Ref.[5] , but for the case of a plane wave diffracting on the cylinder, where heating is very inefficient. The

Further author information: (Send correspondence to A.A.)
A.A.: E-mail: akhmeteli@ltasolid.com, Telephone: +1 310 292 7782
N.G.K.: E-mail: kokodiy.n.g@gmail.com

Cyber Sensing 2014, edited by Igor V. Ternovskiy, Peter Chin, Proc. of SPIE Vol. 9097, 90970H
 · doi: 10.1117/12.2053482

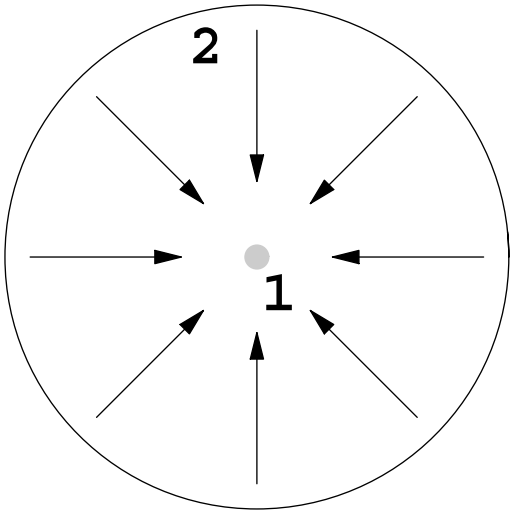

Figure 1. Transverse geometry (the axes of a converging cylindrical wave and a cylinder coincide; there is no energy flow along the axis; the wavelength is considered the transverse dimension of the beam). 1 – cylindrical target; 2 - incident converging cylindrical electromagnetic wave .

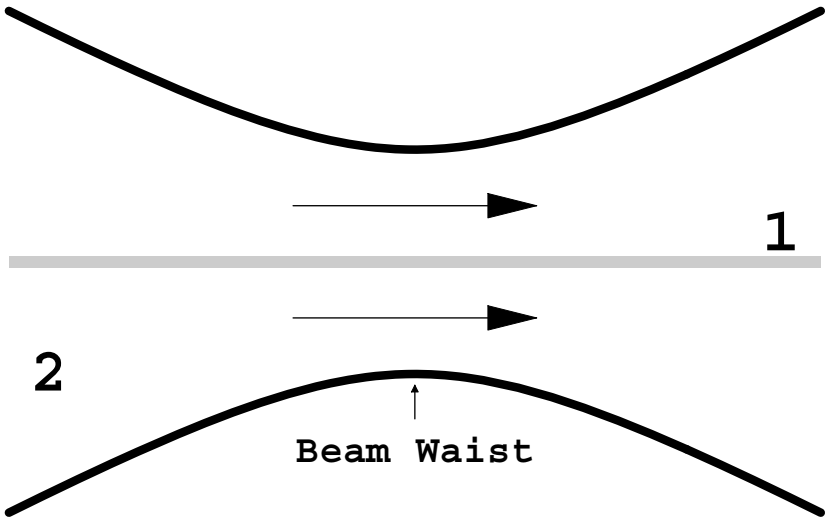

Figure 2. Longitudinal geometry (the axes of a Gaussian beam and a cylinder coincide; the energy flows mainly along the axis). 1 – cylindrical target; 2 – incident Gaussian electromagnetic beam (energy flows from left to right).

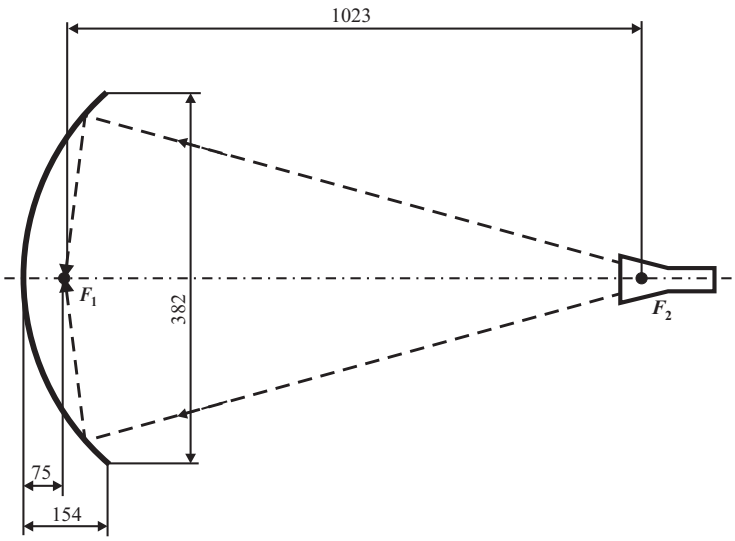

Figure 3. The experimental setup, transverse geometry (not to scale). The dimensions are in millimeters.

experimental results of Ref.[6] , motivated by the theoretical results of work [5] , were obtained for absorption of microwave H_{01} mode at the output of a waveguide, and overall heating efficiency was not assessed. In the present experiment, we demonstrate efficient heating of a thin fiber by an electromagnetic beam in free space, thus confirming the predictions of Refs.[1–3]) (preliminary results for a somewhat problematic configuration were presented in Ref.[9]). The experimental results are in satisfactory agreement (typically up to a factor of 2) with theoretical computations.

The experimental setup is shown schematically in Fig. 3.

A thin wire or fiber is placed in focus F_1 of the ellipsoidal reflector. The internal surface of the reflector is a part of an ellipsoid of revolution defined by the equation:

$$\frac{x^2}{a^2} + \frac{y^2 + z^2}{b^2} = 1, \tag{1}$$

where $a \approx 586$ mm is the major semiaxis and $b \approx 287$ mm is the minor semiaxis of the relevant ellipse. The distance between the foci F_1 and F_2 is approximately 1023 mm. The dimensions of the reflector and the position of focus F_1 inside the reflector are shown in Fig. 3. A horn with aperture 31 x 22 mm^2 and length 130 mm is placed in focus F_2 (the distance between the horn aperture and the focus is 65 mm). The wide side of the horn is horizontal. The horn is connected to a waveguide with dimensions 7.2 x 3.4 mm^2 with mode H_{10}. The frequency of the electromagnetic radiation varied from 24.5 GHz to 39 GHz, and the power varied from 20 mW to 61 mW. Typically, most of the power is collected by the reflector and focused in focus F_1.

In the experiment, microwave absorption in two targets was studied: 1) a platinum wire of diameter 3.5 micron and length ≈25 mm, and 2) a carbon fiber (Thornel P-25 4K, Ref.[10]) of diameter 11 micron and length ≈30 mm. The power absorbed in the cylindrical targets was measured using a method described below (see Methods). The experimental results were compared with the results of computations (see Methods).

For the platinum wire, a tabular value of the temperature coefficient of resistance α_r =0.004 K^{-1} was used, and for the carbon fiber, the value α_r =-0.00021 K^{-1} was found experimentally based on the current-voltage curve.

To determine the linear convection heat transfer coefficient for the fiber, the Joule power for a direct current was calculated based on the measurements of the current and the voltage, and the temperature increase was calculated based on the measured change of the fiber resistivity. The value of the coefficient differed slightly for a vertical and horizontal fiber (cf. Ref.[11]): 0.017 W/(m-K) and 0.019 W/(m-K), respectively. For the platinum wire

of diameter 3.5μ, the following values obtained by N. G. Kokodiy and A. O. Pak (private communication) were used for the vertical and horizontal orientation of the wire: 0.023 W/(m-K) and 0.026 W/(m-K), respectively.

The dependence of absorption of electromagnetic power in the platinum wire on the frequency was measured. This case is not optimal for target heating, so only about 1% of the beam power was absorbed in the wire.

The experimental values were in good agreement with the theoretical ones (see details in arXiv:1109.1626). The wire is heated just by 1K or less, so air flows could significantly influence the results.

The same dependence was measured for the carbon fiber. In this case, significantly more power was absorbed – up to 6%. The experimental values were less than the theoretical ones, but the agreement seems satisfactory (see arXiv:1109.1626).

The discrepancy between theory and experiment may be due to inaccuracies of the fiber positioning or to a discrepancy between conductivity for direct current and for microwave frequencies.

To asses the effect of microwave field polarization on absorption in the fiber, the experiment was conducted for a horizontal orientation of the fiber, when the electric field is orthogonal to the wire. Within our approximations, the theoretical absorption efficiency is zero in this case. The experimental values (less than 0.4%) were much less than for the other polarization, and the specific experimental values were not very reliable, as the fiber resistance changes were comparable to instrument error.

Absorption in the cylindrical target can be significantly greater for an axisymmetric converging cylindrical wave incident on the target. In this case, up to 40% of the incident power can be absorbed in the carbon fiber. The absorption in the platinum wire is significantly less – about 4%.

In this experiment, the absorption is relatively modest – about 6% for the carbon fiber. This is due to the selected configuration. As continuous wave was used in the experiment, care was taken to exclude a possibility of multi-path heating of the target. Electromagnetic radiation reflected from the wire and then from the reflector would be directed to the other focus of the reflector. The absorption efficiency is proportional to the square of the angle from which the incident power is directed on the target. In our experiment, this angle is significantly less than 360° (about 200°), so the efficiency is at least 3 times less than for the axisymmetrical cylindrical wave. However, in fast heating applications, the target can be irradiated from all directions, so higher efficiency can be achieved.

2.1 Methods

To measure the power absorbed by a cylindrical target irradiated by a continuous microwave beam, the target's electrical resistance was measured before and during irradiation. When the wire or fiber in the focus is heated by the radiation, the initial resistance of the wire/fiber R_0 changes by ΔR. The average wire/fiber temperature increase ΔT corresponding to ΔR was calculated as

$$\Delta T = \frac{\Delta R}{\alpha_r R_0}, \tag{2}$$

where α_r is the temperature coefficient of resistance.

On the other hand, the steady state wire/fiber temperature increase depends on the absorbed power P_a and the conditions of heat exchange with the environment. We assume that, after a short transient process, all the power absorbed in the wire/fiber is transferred to the surrounding air through convection (the contribution of conductive heat transfer through the ends of the wire/fiber is relatively small, as the wire/fiber is very thin). According to Newton's law of cooling (Ref.[12]),

$$q" = h(T_s - T_\infty), \tag{3}$$

where q" is the convective heat flux, T_s and T_∞ are the temperatures of the wire/fiber surface and of the ambient air at infinity, respectively, and h is the convection heat transfer coefficient. We assume that temperature is

approximately constant in any transverse section of the wire/fiber, as the latter is very thin, and its thermal conductivity is relatively high. Thus, on average(cf. Ref.[6]),

$$\Delta T = \frac{P_a}{a_p L}, \tag{4}$$

where L is the length of the wire/fiber and a_p is the linear convection heat transfer coefficient. For the carbon fiber of diameter 11μ, this coefficient was measured using a direct current.

It follows from Eqs. (2,4) that

$$P_a = \frac{\alpha_p L}{\alpha_r}\frac{\Delta R}{R_0}. \tag{5}$$

Therefore, the efficiency of absorption of microwave power in the wire/fiber equals:

$$K = \frac{P_a}{P} = \frac{\alpha_p L}{\alpha_r P}\frac{\Delta R}{R_0}, \tag{6}$$

where P is the power in the microwave beam.

Theoretical computations of heating efficiency were performed as follows.

The feed horn fields (incident on the reflector) were computed using the following formulas for the far zone of a pyramidal horn.[13]

If the origin is in the center of the horn aperture, and axes x', y', and z' are directed parallel to the broad sides of the horn, parallel to the narrow sides of the horn, and along the horn axis, respectively, the radial distance, inclination angle, and azimuthal angle of the relevant spherical system of coordinates are r, θ, and φ, respectively. The components of the magnetic field in the far zone are

$$\begin{aligned} H_r(r,\theta,\varphi) &= 0, \\ H_\theta(r,\theta,\varphi) &= -\frac{ik\exp(-ikr)}{4\pi r}\frac{E_0}{\eta} I_1 I_2 \cos(\varphi)(1+\cos(\theta)), \\ H_\varphi(r,\theta,\varphi) &= \frac{ik\exp(-ikr)}{4\pi r}\frac{E_0}{\eta} I_1 I_2 \sin(\varphi)(1+\cos(\theta)), \end{aligned} \tag{7}$$

where the temporal dependence factor $\exp(i\omega t)$ is omitted, E_0 is the amplitude of the electric field in the center of the horn aperture for the dominant mode,

$$\begin{aligned} I_1 = \frac{1}{2}\sqrt{\frac{\pi\rho_2}{k}} \times \\ \left(\exp(ik_x'^2\rho_2/2k)\left(C(t_2')-C(t_1')-i\left(S(t_2')-S(t_1')\right)\right)+\exp(ik_x''^2\rho_2/2k)\left(C(t_2'')-C(t_1'')-i\left(S(t_2'')-S(t_1'')\right)\right)\right), \\ I_2 = \sqrt{\frac{\pi\rho_1}{k}}\exp(ik_y^2\rho_2/2k)\left(C(t_2)-C(t_1)-i\left(S(t_2)-S(t_1)\right)\right), \end{aligned} \tag{8}$$

$C(x)$ and $S(x)$ are the cosine and sine Fresnel integrals, respectively, ρ_1 is the distance from the horn aperture plane to the line of intersection of two opposite broad faces of the horn pyramid, ρ_2 is the distance from the horn aperture plane to the line of intersection of two opposite narrow faces of the horn pyramid,

$$\begin{aligned} t_1' &= \sqrt{\frac{1}{\pi k\rho_2}}\left(-\frac{ka_1}{2}-k_x'\rho_2\right), \\ t_2' &= \sqrt{\frac{1}{\pi k\rho_2}}\left(+\frac{ka_1}{2}-k_x'\rho_2\right), \\ k_x' &= k\sin(\theta)\cos(\varphi)+\frac{\pi}{a_1}, \\ t_1'' &= \sqrt{\frac{1}{\pi k\rho_2}}\left(-\frac{ka_1}{2}-k_x''\rho_2\right), \end{aligned}$$

$$
\begin{aligned}
t_2'' &= \sqrt{\frac{1}{\pi k \rho_2}} \left(+ \frac{k a_1}{2} - k_x'' \rho_2 \right), \\
k_x'' &= k \sin(\theta) \cos(\varphi) - \frac{\pi}{a_1}, \\
t_1 &= \sqrt{\frac{1}{\pi k \rho_1}} \left(- \frac{k b_1}{2} - k_y \rho_1 \right), \\
t_2 &= \sqrt{\frac{1}{\pi k \rho_1}} \left(\frac{k b_1}{2} - k_y \rho_1 \right), \\
k_y &= k \sin(\theta) \sin(\varphi),
\end{aligned}
\tag{9}
$$

a_1 and b_1 are the lengths of the wide and the narrow sides of the horn aperture, respectively, and η is the intrinsic impedance of the media (air).

The reflected fields for the ellipsoidal reflector were estimated using methods of physical optics,[14] as the radii of curvature of the reflector are much greater than the wavelength everywhere. The reflected electric field $\boldsymbol{E}_s$ in a field point is calculated using the following formula (Ref.[14]):

$$
\boldsymbol{E}_s = \frac{1}{2\pi i \omega \varepsilon} \times
\int_{S_0} \left((\boldsymbol{n} \times \boldsymbol{H}_i) \cdot \boldsymbol{\nabla} (\boldsymbol{\nabla} \Psi) + k^2 (\boldsymbol{n} \times \boldsymbol{H}_i) \Psi \right) dS,
\tag{10}
$$

where $\Psi = \exp(-ikR/R)$, R is the distance from the field point to the element of area dS on the reflector, gradient operations in the integrand are referred to the field point as an origin, $\boldsymbol{n}$ is the normal to the reflector surface, S_0 is the geometrically illuminated surface of the reflector, components of the incident magnetic field $\boldsymbol{H}_i$ are defined by Eq. (7), ε is the media permittivity.

Absorption of the reflected field of the ellipsoidal reflector in the wire/fiber in the focus of the reflector was computed using the rigorous solution of the problem of diffraction of electromagnetic field on a homogeneous cylinder (Ref.[15]), which has a simpler form in the case of axisymmetrical field (non-axisymmetrical field is not efficiently absorbed in a very thin cylinder). The field incident on the cylinder (wire/fiber) is described by the electric Hertz vector (Ref.[16]) $\boldsymbol{\Pi}(\rho, \varphi, z) = \{0, 0, \Pi(\rho, \varphi, z)\}$. We use a cylindrical coordinate system ρ, φ, z, where axis z coincides with the axis of the cylinder. We do not use the magnetic Hertz vector as the relevant TE field is not efficiently absorbed in a thin cylinder. Therefore, the reflected field of the ellipsoidal reflector (which is the incident field for the cylinder) is defined by the following expansion of the z-component of the electric Hertz vector into cylindrical waves (Ref.[16]):

$$
\Pi(\rho, \varphi, z) = \int d\gamma \alpha(\gamma) J_0(\lambda_1(\gamma)\rho) \exp(i\gamma z),
\tag{11}
$$

where the limits of integration are $-\infty$ and ∞, $J_n(x)$ is the Bessel function of order n, $\lambda_1^2(\gamma) = \epsilon_1 k_0^2 - \gamma^2$ (it is assumed that magnetic permeabilities of air and the cylinder, μ_1 and μ_2, equal 1), $\epsilon_1 \approx 1$ is the electric permittivity of air, $k_0 = \omega/c$ is the wave vector in vacuum, $\omega = 2\pi\nu$ is the frequency of the electromagnetic field (the factor $\exp(-\omega t)$ is omitted). Function $\alpha(\gamma)$ can be defined as follows. The z-component of the incident electric field corresponding to Eq. (11) can be written as follows:

$$
E_z(\rho, \varphi, z) = \int d\gamma \alpha(\gamma) \frac{\lambda_1^2(\gamma)}{\epsilon_1} J_0(\lambda_1(\gamma)\rho) \exp(i\gamma z),
\tag{12}
$$

so

$$
\alpha(\gamma) \lambda_1^2(\gamma) = E_z(\gamma) = \frac{1}{2\pi} \int dz E_z(z) \exp(i\gamma z),
\tag{13}
$$

where $E_z(z)$ is the z-component of the incident electric field on the axis of the cylinder (where $\rho = 0$ and $J_0(\lambda_1(\gamma)\rho) = 1$), computed using Eq. (10), and $E_z(\gamma)$ is its Fourier transform. Eq. (12) correctly describes the

z-component of the incident electric field in the vicinity of the axis, although Eq. (11) does not include the TE-field and non-axisymmetrical field, which are not efficiently absorbed in the thin cylinder.

The z-component of the electrical Hertz vector of the field refracted in the cylinder can be calculated using the rigorous solution of the problem of diffraction of electromagnetic field on a homogeneous cylinder (Ref.[3, 15]):

$$u_2(\rho,\varphi,z) = \int d\gamma a_2(\gamma) J_0(\lambda_2(\gamma)\rho)\exp(i\gamma z), \tag{14}$$

where

$$\begin{aligned} a_2(\gamma) &= \frac{\alpha(\gamma)\frac{\epsilon_2}{\epsilon_1}\frac{1}{J_0(p_2(\gamma))}\frac{-2i}{\pi p_2^2(\gamma)H_0^{(1)}(p_1(\gamma))}}{-\left(\frac{1}{p_1(\gamma)}\frac{H_0^{(1)'}(p_1(\gamma))}{H_0^{(1)}(p_1(\gamma))} - \frac{1}{p_2(\gamma)}\frac{\epsilon_2}{\epsilon_1}\frac{J_0'(p_2(\gamma))}{J_0(p_2(\gamma))}\right)} = \\ &= \frac{\alpha(\gamma)\epsilon_2\frac{1}{J_0(p_2(\gamma))}\frac{2i}{\pi p_2^2(\gamma)H_0^{(1)}(p_1(\gamma))}}{\frac{1}{p_2(\gamma)}\epsilon_2\frac{J_1(p_2(\gamma))}{J_0(p_2(\gamma))} - \frac{1}{p_1(\gamma)}\frac{H_1^{(1)}(p_1(\gamma))}{H_0^{(1)}(p_1(\gamma))}}, \end{aligned} \tag{15}$$

as $\epsilon_1 \approx 1$ and, for example, $H_0^{(1)'} = -H_1^{(1)}$, $\epsilon_2 = \epsilon = \epsilon' + 4\pi i\sigma/\omega$ is the complex electric permittivity of the cylinder, ϵ' is the real part of the permittivity, σ is the conductivity of the cylinder, $p_1(\gamma) = \lambda_1(\gamma)a$, $p_2(\gamma) = \lambda_2(\gamma)a$, a is the radius of the cylinder, $H_n^{(1)}(x)$ is the Hankel function, $\lambda_2^2(\gamma) = \epsilon_2 k_0^2 - \gamma^2$.

The averaged ρ-component of the Poynting vector at the surface of the cylinder equals

$$\begin{aligned} &\frac{1}{2}\frac{c}{4\pi}\Re\left(\left(\boldsymbol{E}(a,\varphi,z)\times\boldsymbol{H}^*(a,\varphi,z)\right)_\rho\right) = \\ &\quad = -\frac{1}{2}\frac{c}{4\pi}\Re\left(E_z(a,\varphi,z)H_\varphi^*(a,\varphi,z)\right), \end{aligned} \tag{16}$$

as $H_z(a,\varphi,z) = 0$.

The total power absorbed in the cylinder W equals

$$\begin{aligned} &-2\pi a\int dz\left(-\frac{1}{2}\frac{c}{4\pi}\right)\Re\left(E_z(a,\varphi,z)H_\varphi^*(a,\varphi,z)\right) = \\ &\quad = \frac{ac}{4\pi}\int dz\Re\left(E_z(a,\varphi,z)H_\varphi^*(a,\varphi,z)\right) \end{aligned} \tag{17}$$

(an extra minus sign is introduced as positive ρ-component of the Poynting vector corresponds to energy flow out of the cylinder, and we are interested in the absorbed power.) Although the limits of integration are $-\infty$ and ∞, the reflected fields of the ellipsoidal reflector are negligible beyond the focal area. The components of the electric and magnetic field for the electric Hertz vector of Eq. (14) equal

$$\begin{aligned} E_z(a,\varphi,z) &= \int d\gamma a_2(\gamma)\exp(i\gamma z)\frac{\lambda_2^2(\gamma)}{\epsilon_2}J_0(p_2(\gamma)), \\ H_\varphi^*(a,\varphi,z) &= \int d\gamma' a_2^*(\gamma')\exp(-i\gamma' z)(-ik_0)\lambda_2^*(\gamma')J_0^{'*}(p_2(\gamma')), \end{aligned} \tag{18}$$

so

$$\begin{aligned} &\int dz E_z(a,\varphi,z)H_\varphi^*(a,\varphi,z) = \\ &= \int dz\int d\gamma a_2(\gamma)\exp(i\gamma z)\frac{\lambda_2^2(\gamma)}{\epsilon_2}J_0(p_2(\gamma))\int d\gamma' a_2^*(\gamma')\exp(-i\gamma' z)(-ik_0)\lambda_2^*(\gamma')J_0^{'*}(p_2(\gamma')) = \\ &= \int\int d\gamma d\gamma' a_2(\gamma)a_2^*(\gamma')\frac{\lambda_2^2(\gamma)}{\epsilon_2}(-ik_0)\lambda_2^*(\gamma')J_0(p_2(\gamma))J_0^{'*}(p_2(\gamma'))\int dz\exp(i\gamma z)\exp(-i\gamma' z) = \end{aligned}$$

$$= \int\int d\gamma d\gamma' a_2(\gamma) a_2^*(\gamma') \frac{\lambda_2^2(\gamma)}{\epsilon_2} (-ik_0) \lambda_2^*(\gamma') J_0(p_2(\gamma)) J_0^{'*}(p_2(\gamma')) 2\pi\delta(\gamma - \gamma') =$$

$$= 2\pi \int d\gamma a_2(\gamma) a_2^*(\gamma) \lambda_2^2(\gamma) \lambda_2^*(\gamma) \frac{-ik_0}{\epsilon_2} J_0(p_2(\gamma)) J_0^{'*}(p_2(\gamma)), \tag{19}$$

and

$$\Re\left(\frac{-ik_0}{\epsilon_2 \lambda_2^*(\gamma)} J_0(p_2(\gamma)) J_0^{'*}(p_2(\gamma))\right) =$$

$$= \Im\left(\frac{k_0}{\epsilon_2 \lambda_2^*(\gamma)} J_0(p_2(\gamma)) J_0^{'*}(p_2(\gamma))\right) =$$

$$= k_0 J_0(p_2(\gamma)) J_0^*(p_2(\gamma)) \Im\left(\frac{1}{\epsilon_2 \lambda_2^*(\gamma)} \frac{J_0^{'*}(p_2(\gamma))}{J_0^*(p_2(\gamma))}\right) =$$

$$= -k_0 J_0(p_2(\gamma)) J_0^*(p_2(\gamma)) \Im\left(\frac{1}{\epsilon_2^* \lambda_2(\gamma)} \frac{J_0^{'}(p_2(\gamma))}{J_0(p_2(\gamma))}\right). \tag{20}$$

Therefore, Eq. (17) can be rewritten as follows:

$$W = \frac{ac}{4} 2\pi \int d\gamma \left|a_2(\gamma) \lambda_2^2(\gamma) J_0(p_2(\gamma))\right|^2 (-k_0) \Im\left(\frac{1}{\epsilon_2^* \lambda_2(\gamma)} \frac{J_0^{'}(p_2(\gamma))}{J_0(p_2(\gamma))}\right) =$$

$$= \frac{k_0 ac}{4} 2\pi \int d\gamma \left|a_2(\gamma) \lambda_2^2(\gamma) J_0(p_2(\gamma))\right|^2 \Im\left(\frac{1}{\epsilon_2^* \lambda_2(\gamma)} \frac{J_1(p_2(\gamma))}{J_0(p_2(\gamma))}\right), \tag{21}$$

as $J_0^{'}(x) = -J_1(x)$.

The radiated power of the pyramidal horn antenna (in the Gaussian system of units) equals[13]

$$W_0 = \frac{1}{4} \frac{c}{4\pi} a_1 b_1 E_0^2, \tag{22}$$

where a_1 and b_1 are the dimensions of the horn aperture and E_0 is the amplitude of the electric field in the center of the aperture. Therefore, the heating efficiency (the part of the radiated power that is absorbed in the cylinder) equals

$$\frac{W}{W_0} = \frac{8\pi^2 k_0 a \int d\gamma \left|a_2(\gamma) \lambda_2^2(\gamma) J_0(p_2(\gamma))\right|^2 \Im\left(\frac{1}{\epsilon_2^* \lambda_2(\gamma)} \frac{J_1(p_2(\gamma))}{J_0(p_2(\gamma))}\right)}{a_1 b_1 E_0^2}. \tag{23}$$

The following values of resistivity were used for the platinum wire and the carbon fiber, respectively: 0.106 μOhm-m and 13 μOhm-m.

While some manufacturer's data (Ref.[10]) were used in computations for the carbon fiber, the experimental data for the specific fiber were somewhat different. For example, the fiber diameter was measured using diffraction of a broad laser beam on the fiber, and the measured value was 10.1 ± 0.5 micron, rather than 13 micron. The fiber resistivity was determined using measurements of the fiber resistance and dimensions. The value of resistivity was 16 ± 2 μOhm-m, rather than 11 μOhm-m. Using these parameters in computations did not result in significant modifications. For example, the part of power absorbed in the fiber changes from 9.7% to 10.4% at 39 GHz. The computed absorbed power changed insignificantly when the value of the real part of the complex electric permittivity of the fiber changed, e.g., from -1 to 5.

3. LONGITUDINAL GEOMETRY

The experimental setup is shown schematically in Fig. 4.

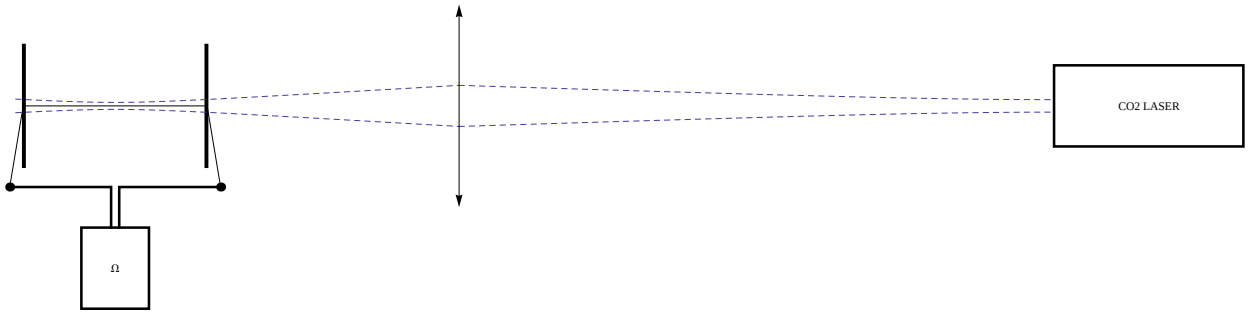

Figure 4. The experimental setup, longitudinal geometry (not to scale).

The CO_2 laser emits infrared radiation (the wavelength λ is 10.6 micron). The thin wire was mounted using crosswires in vertical planes at each end. Each crosswire consisted of two mutually orthogonal thin nickel wires (length – about 60 mm, diameter – 50 micron). The wires were placed at 45° to the vertical. The horizontal wire was placed upon these crosswires and had to be pulled taut to ensure its stability in the course of heating. Previously, a different wire mounting method was used (see the earlier versions of arXiv:1208.0066). The parameters of the horizontal wire are given in Table 1.

Material	D, μm	L, m	α_r, K^{-1}	α_p, W/(m·K)
Pt	20	1.1	$4 \cdot 10^{-3}$	$4 \cdot 10^{-2}$

Table 1. Wire material, diameter D, length L, temperature coefficient of resistance α_r, linear heat exchange coefficient α_p.

The linear heat exchange coefficient depends weakly on the material and the wire diameter in this range of parameters. It was measured through heating the wire with direct current.

The beam is focused by a ZnSe lens (the focal length f is 1700 mm). The electrical resistance of the wire is measured with an ohmmeter. The parameters of the beam and the wire provide efficient absorption for the platinum wire (case 2.1.2.1, Eq. (167) of Ref.[1] , version 1).

3.1 Methods and results

The efficiency of absorption of laser beam power in the wire is calculated using Eq. (6), where L is the length of the wire between the crosswires, and P is the power in the laser beam.

The results of the experiments are presented in Fig. 5.

The measured absorption efficiency was compared to the absorption efficiency of 0.58 computed using the precise theoretical method for a gaussian beam of Refs.[1,3,17]). Thus, the experimental results are in qualitative agreement with the theoretical predictions derived for gaussian beams. It should be emphasized that the efficiency achieved in the experiment is quite high, as the measured width of the beam's waist (1.2 mm at 1/e intensity level) is two orders of magnitude greater than the wire diameter (20 micron).

The exact cause of the nonlinearity (significant dependence of the absorption efficiency on the beam power) has not been established yet, but variation of the air refraction index due to convective flows from the heated wire is a candidate, as the following observation suggests: we directed a laser beam in the visible range along the wire, and the beam's structure (observed on a screen behind the wire) changed when the CO_2 laser beam was switched on and off. No such change of structure was observed when the visible beam was deflected away from the wire.

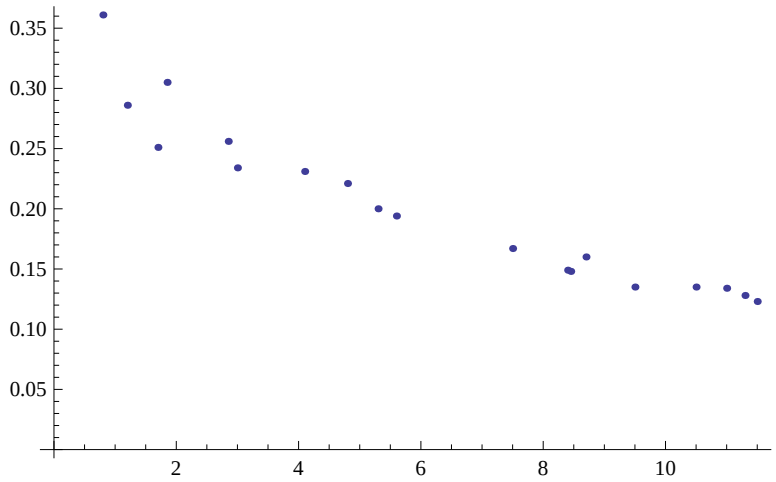

Figure 5. Absorption efficiency vs beam power, W.

4. CONCLUSIONS

The results of the experiments on target irradiation in the transverse and the longitudinal geometries demonstrate the feasibility of efficient heating of thin cylindrical targets with broad electromagnetic beams with transverse dimensions several orders of magnitude greater than the diameter of the target. To this end, there needs to be a match between the diameter of the target, its conductivity, and the wavelength. However, the conditions of efficient heating are non-resonant and therefore very promising for numerous applications. The heating efficiency of tens percent can be achieved for very thin targets.

REFERENCES

[1] Akhmeteli, A., [*Efficient Heating of Thin Cylindrical Targets by Broad Electromagnetic Beams II*], arxiv:physics/0611169 (2006).

[2] Akhmeteli, A. M., "Fast resonatorless hf heating of fusion target," in [*III Inter-Republican Seminar 'Physics of Fast Processes', Grodno*], 4 (1992).

[3] Akhmeteli, A., [*Efficient Heating of Thin Cylindrical Targets by Broad Electromagnetic Beams I*], arxiv:physics/0405091 (2004).

[4] Zharov, A. A. and Zaboronkova, T. M., "Optimum absorption of electromagnetic waves by bounded plasmas," *Soviet Journal of Plasma Physics* **9**, 580 (1983).

[5] Shevchenko, V. V., "On the absorption of Electromagnetic Waves by a Thin Wire," *Soviet Journal of Communications Technology and Electronics* **37(6)**, 121 (1992).

[6] Kuz'michev, V. M., Kokodii, N. G., Safronov, B. V., and Balkashin, V. P., "The efficiency factor for absorption in a metal cylinder in the microwave band," *J. Commun. Technol. Electron.* **48**, 1240 (2003).

[7] Kim, A. V. and Fraiman, G. M., "Nonlinear stage of the thermal-ionization instability in a high-pressure rf discharge," *Soviet Journal of Plasma Physics* **9**, 358 (1983).

[8] Avetisov, V. G., Gritsinin, S. I., Kim, A. V., Kossyi, I. A., Kostinskii, A. Y., Misakyan, M. A., Nadezhdinskii, A. I., Tarasova, N. M., and Khusnutdinov, A. N., "Ionization collapse of rf plasma filament in dense gas," *JETP Lett.* **51**, 348 (1990).

[9] Akhmeteli, A., Kokodiy, N. G., Safronov, B., Balkashin, V., Priz, I., and Tarasevitch, A., [*Efficient Microwave Absorption in Thin Cylindrical Targets: Experimental Evidence*], arxiv:physics/1107.5921 (2011).

[10] Cytec.

[11] Bosworth, R. C. L., [*Heat Transfer Phenomena*], Associated General Publications PTY. LTD (1952).

[12] Incropera, F. P. and DeWitt, D. P., [*Fundamentals of Heat and Mass Transfer*], Wiley (2002).

[13] Balanis, C. A., [*Antenna Theory, 3rd ed.*], Wiley (2005).
[14] Silver, S., [*ed., Microwave Antenna Theory and Design*], P. Peregrinus (1984).
[15] Wait, J. R., "Scattering of a plane wave from a circular dielectric cylinder at oblique incidence," *Can. Journ. of Phys.* **33**, 189 (1955).
[16] Stratton, J. A., [*Electromagnetic Theory*], IEEE-Wiley (2007).
[17] Akhmeteli, A. M. *Soviet Technical Physics Letters* **17(6)**, 396 (1991).